



Contents lists available at ScienceDirect

European Journal of Medicinal Chemistry

journal homepage: <http://www.elsevier.com/locate/ejmech>

Research paper

Structure-based design of allosteric calpain-1 inhibitors populating a novel bioactivity space

Leen Kalash ^{a,1}, Joel Cresser-Brown ^{b,1}, Johnny Habchi ^c, Connor Morgan ^b,
David J. Miller ^b, Robert C. Glen ^{a,d,**}, Rudolf K. Allemann ^{b,***}, Andreas Bender ^{a,*}

^a Centre for Molecular Informatics, Department of Chemistry, University of Cambridge, Lensfield Road, Cambridge, CB2 1EW, United Kingdom^b School of Chemistry, Cardiff University, Main Building, Park Place, Cardiff, CF10 3AT, United Kingdom^c Centre for Misfolding Diseases, Department of Chemistry, University of Cambridge, Lensfield Road, CB2 1EW, United Kingdom^d Integrative Systems Medicine and Digestive Disease, Department of Surgery and Cancer, Faculty of Medicine, Imperial College London, Exhibition Road, London, SW7 2AZ, United Kingdom

ARTICLE INFO

Article history:

Received 28 May 2018

Received in revised form

13 August 2018

Accepted 17 August 2018

Available online 23 August 2018

Keywords:

Allosteric inhibition

PEF(S)

Calpain-1 inhibitors

Structure-based design

Docking

ABSTRACT

Dimeric calpains constitute a promising therapeutic target for many diseases such as cardiovascular, neurodegenerative and ischaemic disease. The discovery of selective calpain inhibitors, however, has been extremely challenging. Previously, allosteric inhibitors of calpains, such as PD150606, which included a specific α -mercaptoacrylic acid sub-structure, were reported to bind to the penta-EF hand calcium binding domain, PEF(S) of calpain. Although these are selective to calpains over other cysteine proteases, their mode of action has remained elusive due to their ability to inhibit the active site domain with and without the presence of PEF(S), with similar potency. These findings have led to the question of whether the inhibitory response can be attributed to an allosteric mode of action or alternatively to inhibition at the active site. In order to address this problem, we report a structure-based virtual screening protocol as a novel approach for the discovery of PEF(S) binders that populate a novel chemical space. We have identified compound **1**, Vidupiprant, which is shown to bind to the PEF(S) domain by the TNS displacement method, and it exhibited specificity in its allosteric mode of inhibition. Compound **1** inhibited the full-length calpain-1 complex with a higher potency ($IC_{50} = 7.5 \mu M$) than the selective, cell-permeable non-peptide calpain inhibitor, PD150606 ($IC_{50} = 19.3 \mu M$), where the latter also inhibited the active site domain in the absence of PEF(S) ($IC_{50} = 17.8 \mu M$). Hence the method presented here has identified known compounds with a novel allosteric mechanism for the inhibition of calpain-1. We show for the first time that the inhibition of enzyme activity can be attributed to an allosteric mode of action, which may offer improved selectivity and a reduced side-effects profile.

© 2018 The Authors. Published by Elsevier Masson SAS. This is an open access article under the CC BY license (<http://creativecommons.org/licenses/by/4.0/>).

1. Introduction

Calpains are proteins that belong to the family of calcium-dependent, non-lysosomal cysteine proteases expressed ubiquitously in mammals and other organisms [1]. Although the physiological roles of calpains are still poorly understood, they have been shown to be involved in many processes such as cell motility, long-term potentiation in neurons and cell fusion in myoblasts [2]. In particular, conventional dimeric calpains have been reported to be involved in the cell degeneration processes that characterize numerous disease conditions [3].

Calpain-1 (μ -calpain) and calpain-2 (m -calpain) are heterodimeric proteases composed of a large subunit with a molecular mass of ~80 kDa, sharing a small subunit of mass ~30 kDa. The small

Abbreviations: PEF(S), penta-EF hand calcium binding domain; TNS, p-toluidinylnaphthalene-6-sulfonate; CysPC, calpain-like protease domain; kDa, kilo Dalton; SAR, structure activity relationship; NR, no response; CNS, central nervous system; HBD, hydrogen bond donor; HBA, hydrogen bond acceptor; tPSA, topological polar surface area; MW, molecular weight.

* Corresponding author.

** Corresponding author. Centre for Molecular Informatics, Department of Chemistry, University of Cambridge, Lensfield Road, Cambridge, CB2 1EW, United Kingdom.

*** Corresponding author.

E-mail addresses: rcg28@cam.ac.uk (R.C. Glen), AllemannRK@cardiff.ac.uk (R.K. Allemann), ab454@cam.ac.uk (A. Bender).

¹ Equal Contribution.

<https://doi.org/10.1016/j.ejmech.2018.08.049>

0223-5234/© 2018 The Authors. Published by Elsevier Masson SAS. This is an open access article under the CC BY license (<http://creativecommons.org/licenses/by/4.0/>).

subunit consists of two domains, namely the penta-EF hand calcium binding PEF(S) and glycine rich (GR) domains, which are essential for stabilizing calpain-1 and calpain-2 [4]. High sequence similarity of 62% is exhibited by the large subunits of calpain-1 and -2 in humans [4]. And they consist of four different domains, an N-terminal anchor helix, the active site domain (CysPc), a domain that resembles the C2 membrane binding domains of phosphokinases, known as the C2L domain, and a second penta-EF hand calcium binding domain known as PEF(L). The PEF(L) domain is the determinant of the calcium concentration that is required for protease activation, which differentiates between the two isoforms: calpain-1 requires micromolar concentrations of Ca^{2+} , whereas calpain-2 requires millimolar concentrations for activation [5].

Calpain-1 is a target dysregulated in many diseases such as neurodegenerative disorders, cardiovascular diseases, ischaemic disorders, arterial sclerosis, leishmaniasis and cancer [6,7]. In most cases of disease, calpain-1 activity is elevated (and hence its inhibition would be beneficial in treatment). However, it has been recently suggested that the up regulation of calpain-1 appears to be beneficial in some cases, such as stage II Alzheimer's disease, where its activation could be neuroprotective and beneficial in controlling cellular damage [8].

Until recently, it has been challenging to design selective calpain-1 inhibitors, and this is attributed to the fact that most compounds that target the active site inhibit a broad spectrum of cysteine proteases, thereby resulting in undesirable side effects [9]. For example, it has been previously reported that calpain-1 inhibitors [9], which also inhibit the proteasome may induce apoptosis, whereas selective calpain-1 inhibitors do not. Hence, it may be beneficial to design selective calpain-1 inhibitors to avoid off-target related side effects.

Classical allosteric inhibitors of calpain-1, which were originally reported to bind to PEF(S), exhibit a very specific type of chemistry – that is α -mercaptoacrylic acid-based, such as PD150606 and PD151746 [10]. These inhibitors are potent, cell permeable and

selective inhibitors of calpain-1 and calpain-2 exhibiting selectivity towards calpain over other cysteine proteases, with a slight selectivity for calpain-1 over calpain-2. It has been reported however that PD150606 could equally inhibit the active site domain of calpain-1 *without* the presence of PEF(S) [11]. This obviously suggests that its mode of action is rather unclear. The reported α -mercaptoacrylic acid based calpain inhibitors (Fig. 1. A. PD150606 and B. PD151746) and their disulfide analogues (Fig. 1. C. and D.) were synthesized by Adams et al., and shown to bind to PEF(S) from X-ray diffraction analysis (PDB IDs: 1NX3, 4WQ2 and 4WQ3) [5,12–14]. Additional calpain-1 inhibitors that were reported to inhibit the whole calpain-1 complex, which consists of the PEF(S) and CysPc (active site domain of calpain-1), are also depicted in Fig. 1, including their chemical structures. CHEMBL203568 [15], shown in Fig. 1. E., is a compound reported to inhibit the calpain-1 complex with an IC_{50} value of 4.9 nM. While CHEMBL204883 [15], shown in Fig. 1. F., is a compound reported to inhibit the calpain-1 complex with an IC_{50} value of 8 nM. However, CHEMBL203568 and CHEMBL204883 have not been confirmed as PEF(S) binders i.e. exhibit an allosteric mode of inhibition. Their reported confidence score is 7 (in ChEMBL) indicating that these compounds might be binding to any of the subunits involved in the full-length calpain-1 complex. Hence, the use of PEF(S) (calpain-1 small subunit) in structure-based virtual screening may be an appealing approach for the design of allosteric calpain-1 binders with completely different structural architecture from the classical allosteric binders and inhibitors. In addition, this approach is expected to answer the question of whether PEF(S) binding would confer inhibition, given that the shortlisting of candidates is based on the prediction of their binding to PEF(S).

In this work, we have used the PEF(S) (PDB ID: 4WQ2, calpain-1 small subunit) in a structure-based virtual screening protocol to ascertain whether novel chemical series bind to the allosteric pocket. To validate this approach, purchasable ligands of diverse and novel structural frameworks (very different from those that

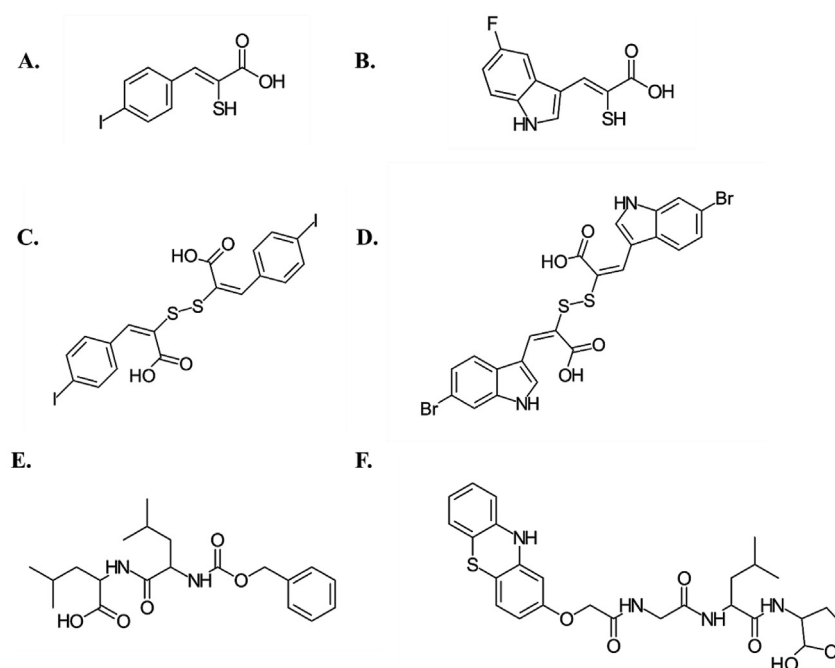


Fig. 1. A. PD150606 B. PD151746 bind to the PEF(S) of calpain, and show modest selectivity for calpain-1 over calpain-2. Adams et al., 2015, synthesized their disulphide analogues C. and D. respectively, which bind to PEF(S) and were reported [5] with improved potencies in comparison to their monomer compounds E. CHEMBL203568, a compound reported to inhibit the calpain-1 complex (Uniprot IDs: P04632 and P07384) with an IC_{50} value of 4.9 nM and confidence score of 7 F. CHEMBL204883, a compound reported to inhibit the calpain-1 complex (Uniprot IDs: P04632 and P07384) with an IC_{50} value of 8 nM and confidence score of 7.

have been previously investigated) were evaluated *in silico*, using ligand/protein docking against PEF(S), and the compounds were subsequently tested in relevant assays. This pipeline for the structure-based virtual screening protocol is depicted in Fig. 2.

As a general approach, we hypothesised that the functional effect of PEF(S) binders on the active site of calpain-1 may be predicted by carrying out Molecular Dynamics (MD) simulations [16,17] on the full-length calpain-1 complex (PEF(S) and CysPc) in both the unbound and the ligand bound states to the PEF(S) domain. If the bound compound increases the average distance between the substrate and the interacting residues in the active site of calpain-1, then we further hypothesise that it would inhibit the activity of the enzyme. In contrast, if the compound decreases this distance, it would favour the interactions between the enzyme and the substrate, thus facilitating the enzyme reaction. A crystal structure of the full-length calpain-1

complex (PEF(S) and CysPc) is currently unavailable, and hence we approached the problem by using the pipeline shown in Fig. 2. Accordingly, the compounds that are predicted to bind to PEF(S) are either expected to inhibit or activate calpain-1.

To explore the small molecule chemical architecture that would most likely alter the geometry of the calpain-1 active site, to inhibit its substrate cleavage allosterically, compounds with diverse chemical structures were investigated computationally based on their predicted binding affinities towards PEF(S). The candidate PEF(S) binders, which were shortlisted by the structure-based virtual screening protocol depicted in Fig. 2 were sulphonamides, N-{3-[3-(2-alkoxyethoxy)-5-(4-methoxyphenyl)]s, and [1,2,4]triazolo [4,3-b]pyridazin-6-yl]pyridines. Experimentally these compounds were also shown to bind to PEF(S) by displacing TNS (which binds to the allosteric site) [10]. In addition, three compounds were able to inhibit the full-length calpain-1 complex (which includes PEF(S) and CysPc) allosterically, but not the active site domain of calpain-1 in the absence of PEF(S). The inhibitory activity, via a proposed allosteric mechanism is a crucial finding given that they show specificity in their mode of action, which is not the case for the classical allosteric inhibitors such as PD150606. The new inhibitors possess different scaffolds from the classical allosteric inhibitors. These compounds serve as a novel starting point for the expansion of the compound series (including SAR) to improve their potency. In addition, this finding suggests that compounds can inhibit the enzyme activity via the PEF(S) domain. An important aspect of this study is that by designing allosteric inhibitors, which do not inhibit the active site domain (that is common to a wide variety of cysteine proteases), these may be effective in treating calpain-1 related diseases without the side effects associated with inhibitors, which do inhibit the active site domain as well [18].

2. Results and discussion

2.1. Structure-based virtual screening of purchasable ligands against PEF(S)

36,503 commercial compounds consisting of diverse chemical structures (sulphonamide-, amide-, pyridine-, urea-, enamine-based compounds), were docked using Glide [19] into the pre-prepared (see methods for details) protein crystal structure of human PEF(S) (PDB [20]ID: 4WQ2) [5]. From the docking scores, the distribution for actives versus inactives was obtained. The active molecules displayed a more favourable distribution of scores, which allowed differentiation of actives and inactives (see methods for details).

Candidate PEF(S) binders from the purchasable database were shortlisted on the basis of a cut-off with the highest Mathews Correlation coefficient. The cut-off obtained was -6.35 , according to which compounds with more negative binding score were predicted to bind. The selected candidates were further screened against PAINS [21] (with regard to the recent analysis of the use of this approach (Tropsha)) [22] using the FAFDrug3 ADME-Tox Filtering Tool [23]. Those compounds that didn't exhibit any potential PAINS liability were considered for evaluation of calpain-1 activity. As a result, five sulphonamides **1–5**, two substituted N-{3-[3-(2-alkoxyethoxy)-5-(4-methoxyphenyl)]s **6–7**, and three substituted [1,2,4]triazolo [4,3-b]pyridazin-6-yl]pyridines **8–10**, which were the top ranked compounds according to the virtual screening criteria, were shortlisted as candidates for PEF(S) binding.

2.2. MDS plot shows that shortlisted PEF(S) binders occupy a novel region in chemical space

An MDS plot of the chemical space was generated consisting of

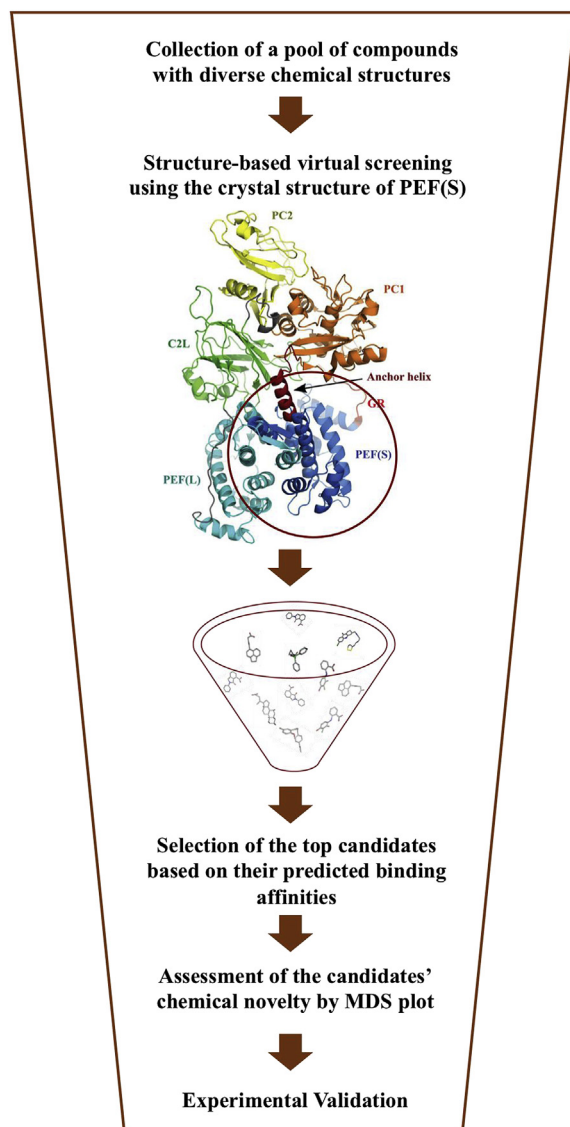


Fig. 2. The pipeline of the structure-based virtual screening protocol followed for shortlisting candidates of PEF(S) binders started with the collection of a pool of compounds with diverse chemical structures (very different from those that have been previously investigated), then candidates were shortlisted based on docking into the crystal structure of PEF(S) (PDB: 4WQ2, calpain-1 small subunit). The top ranked candidates were assessed for their chemical novelty in comparison to the classical allosteric binders and inhibitors using an MDS plot. The subset of compounds was then investigated using relevant experimental assays.

the ChEMBL compounds inhibiting the full-length calpain-1 complex (PEF(S) and CysPc) with IC_{50} values $\leq 1 \mu M$, and the Adams library (a library of α -mercaptoacrylic acid calpain inhibitors and their disulfide analogues) [5], which were validated against the PEF(S) docking model (see methods for details) (Fig. 3). In addition, the shortlisted candidates **1–10** from the structure-based design protocol were also included in the plot, which enabled the assessment of the novelty of chemical space coverage of the shortlisted PEF(S) binders, in comparison to the classical calpain-1 inhibitors and PEF(S) binders. Fig. 3, which is a two dimensional MDS plot based on Morgan fingerprints of radius 2 with 90% ellipse-like confidence regions, shows that the shortlisted compounds **1–10** exhibited new structures in comparison to the previously reported compounds by occupying a novel region in the chemical space of calpain-1 actives.

2.3. FRET based inhibition assay

A fluorogenic assay of the full-length calpain-1 complex (which includes PEF(S) and CysPc) was used to determine the activity of compounds **1–10**. Amongst the identified compounds, **1**, **9**, and **10** inhibited the full-length calpain-1 complex with IC_{50} values of $7.5 (\pm 1.1)$, $20.5 (\pm 1.9)$, and $29.7 (\pm 5.2) \mu M$, respectively (Table 1). The same experimental protocol was performed to measure the activity of compounds against the active site domain of calpain-1, without the presence of PEF(S), to investigate a possible allosteric mode of action. None of the compounds showed any inhibition in the absence of PEF(S), except for compound **1**, which weakly inhibited the active site domain with an IC_{50} value $>100 \mu M$. In contrast, compound **3** exhibited higher inhibitory activity against the active site domain of calpain-1

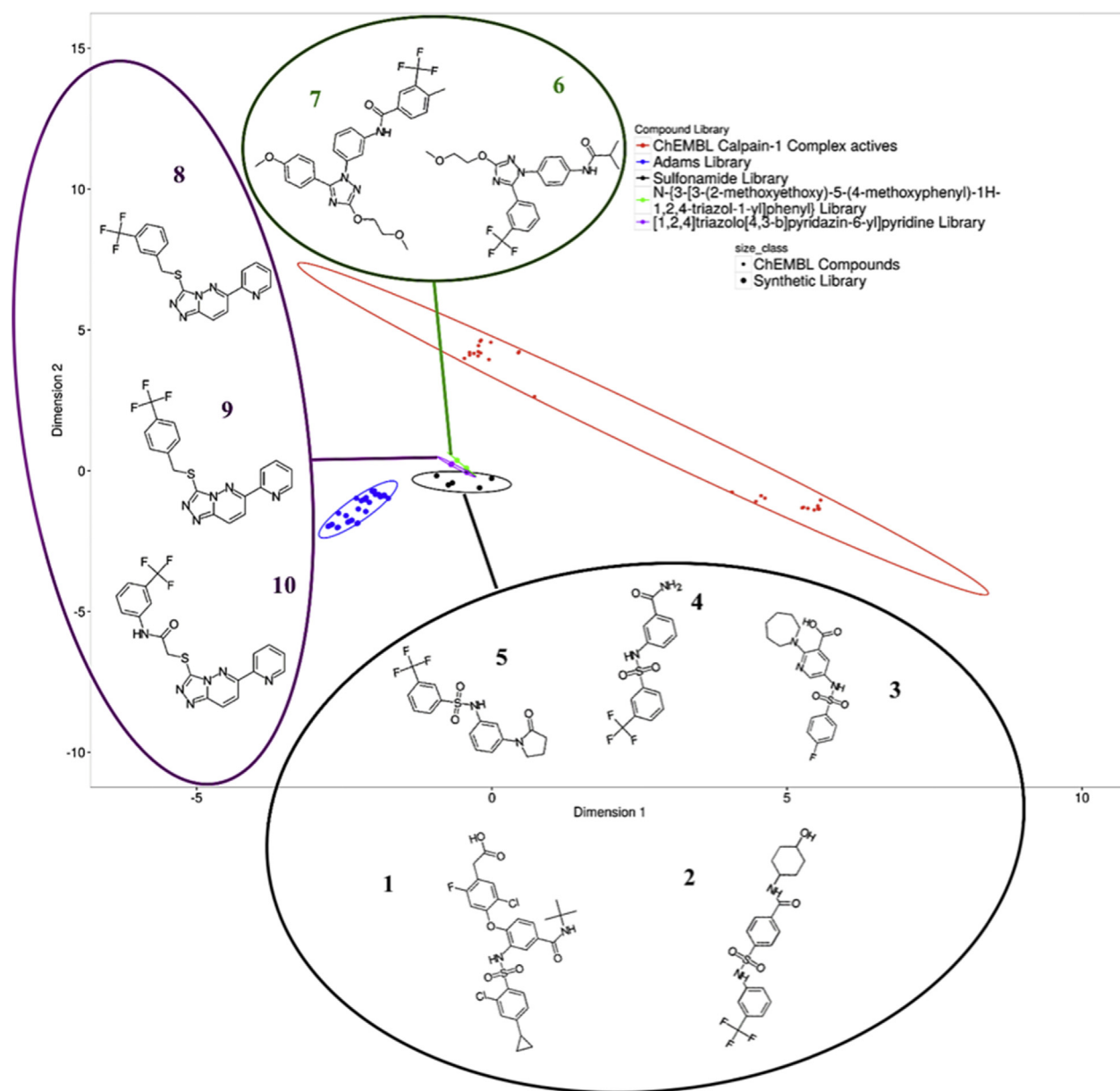


Fig. 3. A two dimensional MDS plot based on Morgan fingerprints of radius 2, with 90% ellipse-like confidence regions for 32 ChEMBL compounds, 33 compounds synthesized by Adams et al., [5] and the 10 shortlisted candidates from the structure-based design protocol. These were shortlisted from a purchasable database based on their high predicted binding affinities towards the PEF(S) domain of calpain via docking with Glide. The compounds identified belong to a new chemical space in comparison to the previously reported compounds that bind to the PEF(S) (Adams library) and the compounds which inhibit the full-length calpain-1 complex. Compounds **1**, **9**, and **10** were then validated as novel allosteric inhibitors of calpain-1.

with an IC_{50} value of $41.1 (\pm 15.4) \mu M$ as compared to the full-length calpain-1 complex, which showed an activity of $>100 \mu M$, suggesting that in the presence of PEF(S) it preferentially binds to PEF(S). This could explain the reduction in its inhibitory activity since it is most likely unable to alter the geometry of the active site while it binds allosterically. The IC_{50} values were also measured for the classical α -mercaptoacrylic acid based calpain inhibitor, PD150606, and these were $19.3 (\pm 1.6) \mu M$ with the full-length calpain-1 complex, and $17.8 (\pm 2.4) \mu M$ with the active site domain without the presence of PEF(S). Hence, in contrast to compounds **1**, **3**, **9**, and **10**, PD150606 exhibited an unspecific mode of action by equally inhibiting via both binding sites (active and allosteric sites). It is worth stating here that compound **1** is an asthma drug, Vidupirant or AMG 853 [24], which exhibited higher potency than PD150606 in inhibiting the enzyme activity. The dose response curve of compound **1** ($IC_{50} = 7.5 \pm 1.1 \mu M$) is displayed in Figure S1. Interestingly, identifying Vidupirant as an allosteric inhibitor of calpain-1 is in agreement with previous reports showing a direct link between calpain inhibition and anti-inflammatory properties, where it was shown that non-steroidal anti-inflammatory drugs (NSAIDs) inhibit calpain, and that calpain inhibition reduces allergic inflammation [25,26]. Potentially, this finding could highlight the importance of considering calpain inhibitors for the development of new anti-asthmatic therapies.

The allosteric inhibitory activity exhibited by compounds **1**, **9**, and **10** validates the design approach, which shortlisted PEF(S) binders. The three active compounds include scaffolds, which are distinct from the classical allosteric inhibitors. The IC_{50} values obtained could be improved by efficient choice of substituents using standard medicinal chemistry approaches. In particular compound **1**, which is a sulphonamide, exhibited specificity in its allosteric inhibition of calpain-1, and was more potent ($7.5 \mu M$) than PD150606 ($19.3 \mu M$), which additionally inhibits the active site domain, in the absence of PEF(S), with a similar IC_{50} value.

2.4. TNS displacement assay

TNS, which is a sensitive fluorophore that binds to PEF(S) was used to probe protein dynamics and conformational change. It fluoresces in the bound state i.e. in a hydrophobic environment, whereas when another compound displaces it, its fluorescence gets quenched. This fluorophore was used previously to assess the binding of PD150606 to PEF(S), a compound which has been already shown to bind to PEF(S) by X-ray crystallography (PDB ID: 1NX3) [10,12]. In this work, PD150606 (as a control), compound **1**, the most potent allosteric inhibitor, compound **3**, a weak allosteric inhibitor, and compounds **2**, **4** and **5**, which did not exhibit any inhibitory activity, have been tested for PEF(S) binding by the TNS displacement method. The results for compounds **6–10** were unreliable as it became apparent that they fluoresced under the assay conditions, therefore for this reason these results were omitted. As shown in Fig. 4, all tested compounds, except for compound **5**, quenched the fluorescence of TNS, exhibiting a similar trend in their quenching effect to that of the known PEF(S) binder, PD150606, hence confirming their binding to PEF(S). Therefore, it appears that compounds **2–4** do indeed bind to PEF(S) in a similar fashion to compound **1**, but they either weakly inhibited or failed to allosterically alter the geometry of the active site.

2.5. Analysis of molecular docking studies of representative calpain-1 inhibitors **1** and **10**, and compounds **2–5**

Docking studies predicted molecular interactions of the

sulphonamide **1** and the [1,2,4]triazolo [4,3-b]pyridazin-6-yl pyridine **10** with the PEF(S) protein crystal structure (PDB ID: 4WQ2). Fig. 5. A. shows the 2-chloro-4-cyclopropylsulfonamido phenyl ring of compound **1** is π -stacked with His₁₃₁, and the carbonyl of its carboxylic acid moiety H-bonds with the same residue, the carbonyl of its amide moiety H-bonds with Trp₁₆₈, and the phenyl ring attached to the tert-butylcarbamoyl moiety is π -stacked with the same residue. Fig. 5. B. shows a π -stacking interaction between the pyridine ring of compound **10** and Trp₁₆₈, and H-bonding of the nitrogen in that ring with the same residue. The hydrophobic interactions predicted for compounds **1** and **10** with Trp₁₆₈ are also seen in the co-crystallised ligand/protein crystal structure (PDB ID: 4WQ3) [5]. In addition, a more favourable binding affinity towards PEF(S) was predicted for compound **1** ($IC_{50} = 7.5 \pm 1.1 \mu M$) as compared to compound **10**, ($IC_{50} = 29.7 \pm 5.2 \mu M$), which could be the reason for the higher inhibitory activity exhibited by compound **1**. In order to further explore the activities of compounds **1–10**, MD simulations on the full-length calpain-1 complex, which includes the PEF(S) domain would be beneficial once the crystal structure is available. The inhibitory activity of each compound is predicted to correlate with the average distance between the substrate and the interacting residues in the active site of calpain-1.

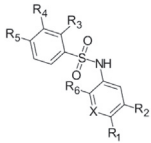
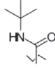

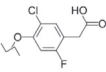
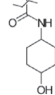
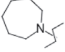
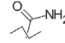
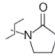
Docking studies predicted molecular interactions of the sulphonamides **2–5** with the PEF(S) protein crystal structure (PDB ID: 4WQ2), which suggest that the hydrophobic interactions with Trp₁₆₈ are essential for PEF(S) binding. Fig. 6. A. shows that the phenyl ring of compound **2**, which is attached to the sulfonyl moiety is π -stacked with Trp₁₆₈, and the same residue H-bonds with the carbonyl of the amide group, the hydroxyl of its cyclohexyl ring H-bonds with Gln₁₀₀, and its sulfonyl group H-bonds with His₁₃₁. Fig. 6. B. displays the predicted molecular interactions between compound **3** and the PEF(S) crystal structure, and these are H-bonding between its carboxyl moiety and the Lys₁₇₂ and Trp₁₆₈ residues, H-bonding between its sulfonyl group and His₁₃₁, and π -stacking with the Trp₁₆₈ via its pyridine ring. Fig. 6. C. demonstrates the predicted molecular interactions for compound **4**, the amino group of its amide moiety H-bonds with the Glu₉₇ and Trp₁₆₈ residues, the phenyl ring of its benzamide group π -stacks with Trp₁₆₈, and the carbonyl of its amide moiety H-bonds with Lys₁₇₂. Fig. 6. D. shows the H-bonding interactions predicted for the carbonyl of the oxopyrrolidin-1-yl moiety in compound **5** and the Lys₁₇₂ and Trp₁₆₈ residues, and H-bonding interactions for its sulfonyl moiety with His₁₃₁, and π -stacking of the same residue with the aromatic ring of its trifluoromethylphenyl moiety. Hence, the hydrophobic interactions predicted for compounds **1–4** with Trp₁₆₈ are also seen in the co-crystallised ligand/protein crystal structure (PDB ID: 4WQ3) [5]. However, compound **5** was predicted to exhibit hydrophilic interactions with Trp₁₆₈, which could explain why it didn't displace TNS, suggesting that the hydrophobic interactions with this residue are essential for PEF(S) binding.

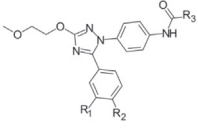
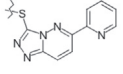
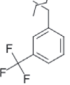
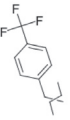
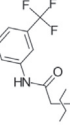
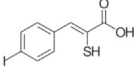
2.6. Computational assessment of CNS permeability for representative calpain-1 inhibitors **1** and **10**

Given that calpain-1 may serve as a therapeutic target for neurodegenerative disorders, the computational assessment of the CNS permeability for compounds **1** and **10** was performed with FAFDrug3 [23] to see whether these compounds could be considered as good starting points to target these diseases. Their physicochemical properties were calculated using FAFDrug3. Following this, CNS diagrams were obtained and are presented in Figure S2. A and B. Compound **1** did not pass the CNS filter, which takes into consideration the assessment of its ability to pass the

Table 1

IC₅₀ values for compounds **1–10**, and PD150606 determined by the FRET based inhibition assay, with the full-length calpain-1 complex and the active site domain of calpain-1, reported as mean \pm standard deviations from three independent experiments (NR = no response).

Compound	Common Scaffold	Substituents	IC ₅₀ full-length calpain-1 complex (μ M)	IC ₅₀ active site domain calpain-1 (μ M)
1		R ₁ and R ₄ = H  R ₂ = R ₃ = Cl  R ₅ =  R ₆ = X = C	7.5 \pm 1.1	>100
2		R ₁ , R ₃ , R ₄ , and R ₆ = H R ₂ = CF ₃  R ₅ = X = C	NR	NR
3		 R ₁ = R ₂ = CO ₂ H R ₃ , R ₄ , and R ₆ = H R ₅ = F X = N	> 100	41.1 \pm 15.4
4		R ₁ , R ₃ , R ₅ and R ₆ = H  R ₂ = R ₄ = CF ₃ X = C	NR	NR
5		R ₁ , R ₃ , R ₅ and R ₆ = H  R ₂ = R ₄ = CF ₃ X = C	NR	NR

6		$R_1 = \text{CF}_3$ $R_2 = \text{H}$ $R_3 = \text{tert-butyl}$	NR	NR
7		$R_1 = \text{H}$ $R_2 = \text{OCH}_3$ $R_3 = \text{4-(tert-butyl)phenyl}$	NR	NR
8			NR	NR
9			20.5 ± 1.9	NR
10			29.7 ± 5.2	NR
PD150606			19.3 ± 1.6	17.8 ± 2.4

blood brain barrier. Hence, it is predicted not to exhibit the desired permeability [27], since the values of all the descriptors for compound **1** (logP, HBD, HBA, MW, tPSA (blue line)) fall outside the CNS filter area (light blue). As for compound **10**, it is predicted to exhibit medium permeability since all the descriptors, except for the HBA, have passed the CNS filter. Hence, compound **10** might serve as a good starting point for analogue development to target neurodegenerative diseases.

3. Conclusions

In this work, we have successfully validated our structure-based design method, which has led to the discovery of chemically novel allosteric inhibitors of calpain-1, and we have shown for the first time an allosteric mode of action. Compounds **1**, **9**, and **10** inhibited the full length calpain-1 complex (which includes PEF(S) and CysPc) with IC_{50} values of 7.5 (±1.1), 20.5

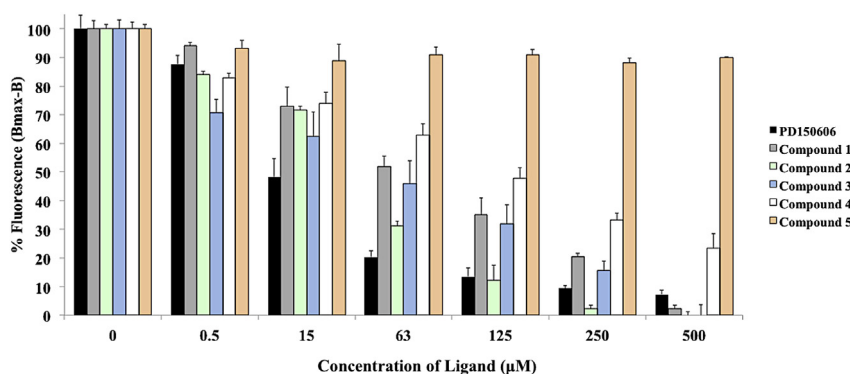


Fig. 4. PD150606, which was shown by X-ray crystallography to bind to PEF(S) (PDB ID: 1NX3), compound **1** (the most potent allosteric inhibitor), **3**, which was the least potent among the identified allosteric inhibitors, **2** and **4**, which did not exhibit any inhibitory activity, all quenched the fluorescence of TNS. All compounds showed a similar effect to that of PD150606 confirming their binding to PEF(S), except for compound **5**, which neither exhibited any inhibitory activity nor displaced TNS.

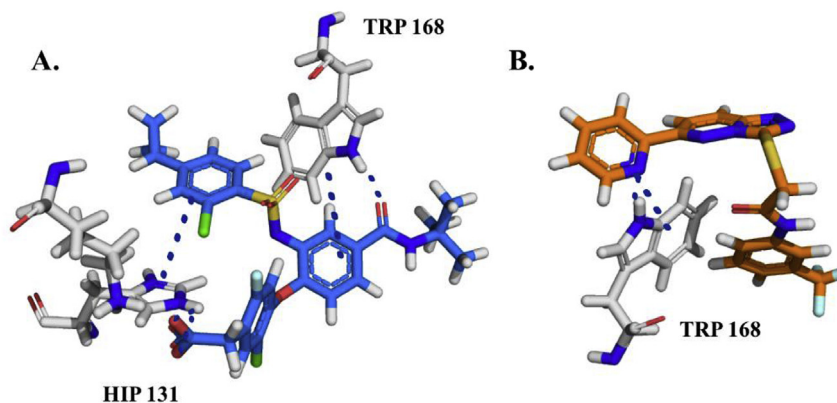


Fig. 5. Docking studies predicted molecular interactions of compounds **1** and **10** with the human PEF(S) of calpain-1 small subunit (regulatory subunit) protein crystal structure (PDB ID: 4WQ2). **A.** The 2-chloro-4-cyclopropylsulfonamido phenyl ring of compound **1** shows π -stacking with His₁₃₁ and the carbonyl of its carboxylic acid moiety H-bonds with the same residue. The carbonyl of its amide moiety H-bonds with Trp₁₆₈ and the phenyl ring attached to the tert-butylcarbamoyl moiety is π -stacked with the same residue **B.** The pyridine ring of compound **10** is π -stacked with Trp₁₆₈ and the nitrogen of that ring H-bonds with same residue. The hydrophobic interactions of **1** and **10** with Trp₁₆₈ are also seen in the co-crystallised ligand/protein crystal structure (PDB ID: 4WQ3) [5].

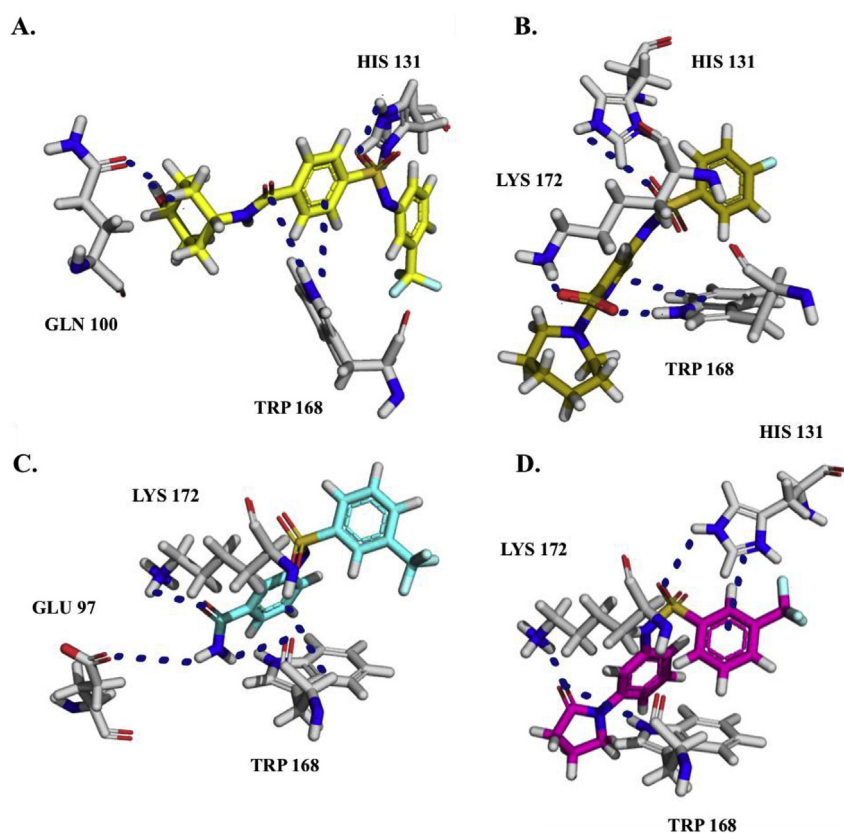


Fig. 6. Docking studies predicted molecular interactions of the sulphonamides **2–5** with the PEF(S) protein crystal structure (PDB ID: 4WQ2), which suggest that hydrophobic interactions with Trp₁₆₈ are essential for PEF(S) binding **A.** The phenyl ring of compound **2**, which is attached to the sulfonyl moiety is π -stacked with Trp₁₆₈, and the same residue H-bonds with the carbonyl of its amide group, the hydroxyl of its cyclohexyl ring H-bonds with Gln₁₀₀, and its sulfonyl group H-bonds with His₁₃₁ **B.** H-bonding interactions are predicted to occur between the carboxyl moiety of compound **3** and the Lys₁₇₂ and Trp₁₆₈ residues, H-bonding between its sulfonyl group and His₁₃₁, and π -stacking with the Trp₁₆₈ via its pyridine ring **C.** The amino group of the amide moiety for compound **4** H-bonds with Glu₉₇ and Trp₁₆₈, and the phenyl ring of its benzamide group π -stacks with Trp₁₆₈, and the carbonyl of its amide moiety H-bonds with Lys₁₇₂ **D.** H-bonding interactions are predicted to occur between the carbonyl of the oxo-pyrrolidin-1-yl moiety for compound **5** and the Lys₁₇₂ and Trp₁₆₈ residues, H-bonding between its sulfonyl moiety and His₁₃₁, and π -stacking of the same residue with the aromatic ring of its trifluoromethylphenyl moiety.

(± 1.9), and 29.7 (± 5.2) μM respectively. Compounds **9** and **10** did not inhibit the active site domain of calpain-1 in the absence of PEF(S), and compound **1** inhibited the active site domain weakly with an IC_{50} value $>100 \mu\text{M}$. In contrast, compound **3** exhibited higher inhibitory activity against the active site domain of

calpain-1 with an IC_{50} value of 41.1 (± 15.4) μM as compared to the full-length calpain-1 complex, which was $>100 \mu\text{M}$ suggesting that it preferentially binds to PEF(S). In addition, the IC_{50} values were measured for PD150606, giving 19.3 (± 1.6) μM with the full-length calpain-1 complex and 17.8 (± 2.4) μM with the

active site domain (without the presence of PEF(S)). In comparison to the classical α -mercaptoacrylic acid based calpain inhibitor, PD150606, compounds **1**, **9**, and **10**, exhibited specificity in their allosteric mode of action, since they didn't inhibit the active site domain in the absence of PEF(S).

Furthermore, PD150606, compound **1**, the most potent allosteric inhibitor, compound **3**, a weak allosteric inhibitor, and compounds **2** and **4**, (which did not exhibit any inhibitory activity) have been tested for PEF(S) binding by the TNS displacement method. All compounds (**1–4**) quenched the fluorescence of TNS, exhibiting a similar trend in their quenching effect to that of the known PEF(S) binder, PD150606.

IC₅₀ values obtained for compounds **1**, **9**, and **10** may be good starting points for optimisation, having novel scaffolds. Allosteric inhibitors discovered by this approach could exhibit more selectivity towards calpain-1 since they are unlikely to inhibit the active site domain, which is similar for a wide variety of cysteine proteases. This could translate to more effective treatments with less side effects for calpain-1 related diseases [18].

4. Materials and methods

4.1. Extracting purchasable compounds for structure-based virtual screening against PEF(S), the calpain small subunit 1 (regulatory subunit)

Purchasable compounds (36,503) with diverse chemistry (sulphonamide-, amide-, pyridine-, urea-, enamine-based compounds), were downloaded from the Aldrich market select database-2016 [28].

4.2. Ligand preparation

The entire set of extracted ligands were prepared for docking with LigPrep 2.5 [29] using the default settings and the Epik option, which introduces energy penalties associated with ionization and tautomerization [30].

4.3. Receptor preparation of PEF(S)

Docking with Glide [19] was performed against human PEF(S), calpain-1 small subunit (regulatory subunit) of the protein crystal structure (PDB [20] ID: 4WQ2) [5] bound to (Z)-3-(6-bromondol-3-yl)-2-mercaptoacrylic acid. The structure was prepared using the protein preparation wizard of Maestro 9.3 [29], following the default protocol, which accounts for energy refinement, hydrogen addition, pK_a assignment, and side-chain rotational isomer refinement. Resolved water molecules were discarded and the structure was centred using the co-crystallised ligand as the centre of the receptor grid generated for the protein structure. The co-crystal structure of the human calpain PEF(S) protein crystal structure (PDB ID: 4WQ2) bound to (Z)-3-(6-bromondol-3-yl)-2-mercaptoacrylic acid was selected as the target structure.

4.4. Cut-off generation for compound selection from docking model

In an attempt to validate the docking model, a set of known active and inactive compounds were docked against the PEF(S) protein crystal structure to ensure that it enriched actives. 32 ChEMBL [31] compounds with IC₅₀ values $\leq 1 \mu\text{M}$ (protein complex of the calpain-1, catalytic and small regulatory subunits: P07384, P04632 with confidence scores of 6 or 7) were docked against the PEF(S) model. In addition, 20 inactive compounds from PubChem [32] of the PEF(S) calpain-1 small regulatory subunit (Uniprot ID: P04632) were docked.

A good separation was obtained for the medians of docking score distribution for actives versus inactives for the docking model indicating that the actives are enriched. Figure S3. shows the separation of the medians for the PEF(S) docking model, -7.48 (actives) vs. -4.60 (inactives). In addition, the indole and the phenyl α -mercaptoacrylic acid-based inhibitors and their disulfide analogues, which were synthesized by Adams et al., [5] and shown by X-ray crystallography to bind to PEF(S), were docked against the PEF(S) docking model. The median of the docking score distribution obtained is -7.25 in comparison to the median of inactives, which is -4.60 (Figure S4., supporting information), which further validates that the model enriches these set of actives. Mann-Whitney test, which included statistical analysis on the active and inactive docking score distributions, was performed with R [33] using the script provided by Kalash et al. [34] The differences in the medians was significant with p values less than 0.05.

The Matthews correlation coefficient (MCC), which takes into account true and false positives and negatives, was computed using a Python script [34] for all the docking scores of the ChEMBL actives and PubChem inactives for the model. A search was performed for a docking score threshold that gave the highest MCC for the docking model in order to shortlist purchasable candidates of PEF(S) binders, which displayed docking scores that are lower than that with the highest MCC for the PEF(S) docking model (which was -6.35).

4.5. Docking

The purchasable compounds, prepared according to the protocol described, were docked against the PEF(S) protein crystal structure (PDB ID: 4WQ2). The Glide docking parameters included extra precision (XP) and the flexible ligand sampling option. These were deduced from docking experiments using known actives and inactives against the protein model. The highest ranked compounds with respect to predicted affinities towards PEF(S) were selected for binding assessment and calpain-1 activity evaluation i.e. those which displayed docking scores that are lower than that with the highest MCC for the PEF(S) docking model, which was -6.35 . The compounds that did not exhibit potential PAINS [21,22] liabilities upon virtual screening with the FAFDrug3 ADME-Tox filtering tool, were selected for experimental validation [23]. The shortlisted compounds exhibited diverse structures, with five sulphonamides **1–5**, two substituted N-{3-[3-(2-alkoxyethoxy)-5-(4-methoxyphenyl)s **6–7**, and three substituted [1,2,4]triazolo [4,3-b]pyridazin-6-yl]pyridines **8–10**.

4.6. Multi-dimensional scaling (MDS) analysis of the shortlisted compounds 1-10

This step of the analysis aimed to plot the chemical space of ChEMBL compounds, which are active against the full-length calpain-1 complex, with IC₅₀ values $\leq 1 \mu\text{M}$ (protein complex of calpain-1, catalytic and small regulatory subunits: P07384, P04632 and confidence scores of 6 or 7), and the Adams library [5], which were validated against the PEF(S) docking model. In addition, the shortlisted candidates from the structure-based design protocol were included in the same plot. This analysis enables an assessment of the novelty of the chemical space coverage of the shortlisted compounds **1–10**. For this purpose, the SMILES of all compounds involved were standardized using the ChemAxon Command-Line Standardizer, where the following options were selected: "Remove Fragment" (keep largest), "Neutralize", "RemoveExplicitH", "Clean2D", "Mesomerize" and "Tautomerize" [35].

Subsequently, Morgan fingerprints (radius 2, 1024 bits) were generated for all the compounds using KNIME 2.11.3 [36]. The

workflow generated Morgan fingerprints in the following sequence: It (a) read chemical data from an SDF file, (b) generated RDKit molecules from a molecule string representation (SDF), (c) generated hashed bit-based fingerprints for an input RDKit Mol column (d) converted RDKit molecules into string based molecule representations (SDF or smiles) (e) excluded columns from the input table (f) renamed columns (g) and saved data table into a CSV file.

A 2D-similarity matrix based on Euclidean distance was computed with R, using the generated Morgan fingerprints. Then, a metric multidimensional scaling of the similarity matrix was computed by embedding it into two dimensions ($k=2$). Subsequently, a 2D-plot was obtained, with the x-axis and the y-axis labelled, Dimension 1 and Dimension 2 respectively. These are two relative and unit-less dimensions that recapitulate the pairwise similarity of all points observed in the distribution of Euclidean distances in a lower dimensional space. For each data set in the plot (corresponding to Adams library, ChEMBL compounds, and the shortlisted compounds), 90% confidence ellipses were computed using the ellipse package. Finally, based on the generated Morgan fingerprints, an MDS plot with 90% ellipse-like confidence regions was obtained using the R ggplot2 package [37].

4.7. Expression and purification of PEF(S)

The codon optimised gene encoding human PEF(S) was purchased from Epoch Biolabs (Texas, USA) in a pET21d vector. Human PEF(S) was produced in *E. coli* BL21-CodonPlus (DE3)-RP (Agilent Technologies), and purified using the same procedure previously described for PEF(S) [5].

4.8. Evaluating calpain-1 activity of the shortlisted candidates of PEF(S) binders 1–10

This assay uses a fluorogenic peptide from the calpain-1 substrate α -spectrin, containing a FAM-DABCYL FRET pair (H_2N -K(-FAM)-EVYGMK(DABCYL)-OH). Cleavage by calpain-1 occurs between the Tyr-Gly residues and results in enhanced fluorescence as the quenching effect is relieved. The assays using purified porcine calpain-1 (CalBiochem, 25 nM) were performed in a buffer containing 1 μ M calpain-1 substrate, 10 mM HEPES, 10 mM DTT, 0.5 mM EDTA, bovine serum albumin (0.1%) pH 6.8. The assay was carried out using a fluorescent plate reader (BMG Optistar) with a final assay volume of 100 μ l at a temperature of 37 °C, using an excitation band pass filter centred at 490 nm and emission detected at 520 nm. The compounds were added to the assay mixture before the reaction was initiated by the addition of $CaCl_2$ (5 mM). None of the compounds had significant fluorescence at this wavelength. The compounds were dissolved in DMSO at 40 mM and diluted into assay buffer to give range of concentrations from 5 nM to 200 μ M. In each assay run, the effect of DMSO alone over the concentration used was also measured. Although there was no effect of DMSO at lower concentrations, in some assay runs, DMSO at 0.005%–0.5% produced some inhibitory effect. This DMSO effect (which was only relevant for compounds with poor inhibitory ability) was subtracted before constructing the inhibition curves [5]. The IC_{50} values were obtained by fitting the data with non-linear regression with the SigmaPlot software [38], and the reported results are the mean \pm standard deviation of three independent experiments.

4.9. TNS displacement for compounds 1–5

10 μ M PEF(S) in 20 mM Tris base, 1.1 mM $CaCl_2$, 1 mM EDTA and pH 7.4 was incubated with 46.7 μ M 2-p-toluidinylnaphthalene-6-sulfonate (TNS, 1 mM stock in 40% ethanol) in a Greiner CELLSTAR

96 well black flat bottom plate for 5 min at 25 °C.

Compounds 1–10 were stored as 40 mM stock solutions in DMSO, then diluted from 500 μ M to 500 nM by serial dilution over 10 wells with an Integra Viaflow 96 multichannel pipette in triplicate.

The plates were then incubated in a FLUOstar Omega plate reader at 25 °C for 5 min then were analysed using an excitation wavelength of 355 nm and an emission wavelength of 450 nm with 10 flashes per well with orbital averaging.

The baseline (just TNS) was subtracted from the fluorescence (B). B was then subtracted from the B_{max} (with no inhibitor) to invert the data. The data was plotted in excel as bar diagrams for the mean \pm standard deviation of three independent experiments ($n=3$) in triplicate as shown in Fig. 4. Whereas for compounds 6–10, their fluorescence interfered with TNS (refer to Figure S5, for the blanks obtained for compounds 1–10), for this reason their results were omitted.

Compounds and reagents Compound 1 was purchased from Tocris, and compounds 2–10 were purchased from Ambinter, and used without further purification. PD150606 was purchased from Sigma-Aldrich and used without further purification.

4.10. Cloning of CysPC gene

The pET28a-GB1-MAAKLVFF plasmid, a kind gift from Dr Cornelius Krasel of the Institut für Pharmakologie (Marburg, Germany), was used to create a Golden Gate acceptor plasmid by standard PCR, overlap extension PCR, endonuclease digestion and T4 DNA ligase reactions. When subjected to Golden Gate digestion/ligation with BsaI and T4 DNA ligase with an appropriate complementary PCR product, the resulting plasmid has a section of DNA encoding RF under a constitutive promoter removed and the PCR product is incorporated in such a fashion that the translation product contains the protein of interest with an N-terminal hexahistidine tag GB1 fusion tag that can be removed by the action of tobacco etch virus protease (TEV).

Digestion/ligation proceeds as expected despite the presence of an additional BsaI site within the sequence encoding RFP. The CysPC domain of calpain-1 was inserted into this acceptor by PCR with the following primers:

Fwd: CGACTAGTGGTCTCCAGTCCATGGGTCGCCATGAGAA

Rev: CGACTAGTGGTCTCCATCAGTCCGGGGTCAGGTTACA for ligation using the golden gate protocol into the pET28a-GB1-MAAKLVFF plasmid [39].

4.10.1. Plasmid sequencing

4.10.1.1. 17 fwd. TAGAAATAATTTTGTTAACTTTAAGAAGGAGATATACCATGGGCAGCAGCCATCATCATCATCACACTTACAAATTAATCCTTAATGGTAAAACATTGAAAGGCCGAAACAACACTACTGAAGCTGTTGATGCTGCTACTGCAGAAAAAGTCTTCAAACAATACGCTAACGACAACGGTGTTGACGGTGAATGGACTTACGACGATGCGACTAAGACCTTACAGTTACTGAACATATGGAAAACCTGTATTTTCACTCCGAGACCTTTACGGCTAGCTCAGCCCTAGGTATTATGCTAGCTACTAGAGAAAGAGGAGAAAACTAGTAGTGTAGCAAAAGCGAGGAGCTGATTAAGGAGAATATGCACATGAACCTGTAGCAAGGCACCGTGAACAACCACTTCAAGTGACCCAGCGAGGTGAAGGCAAACCGTATGAAGGCACCCAGACCATGCGTATCAAGTGGTTAGGGTGGCCCGTCCCGTTCCGTTTGATATTCTGGCGACGAGTTTCATGTACGGTAGCCGTACCTTTATCAACCACCCAGGGCATTCCGGATTCTTTAAACAGAGCTTCCCGGAAGGTTTACCTGGGAGCGGTGACCACTACGAAGACGGTGGCGTTCTGACCGCGACCCAGGACACCAACCTGCAAGATGGCTGCTGATCTATAACGTGAAGATTCGTGGTGTAACTTCCGAGCAACCGCCCGTGAAGAAGAAACCTGGGTGGGAGGCGAACACCGAAATGCTGTATCCGGCGGATGGTGGCCTGGAGGGCGTAGCGACATGGCGCTGAAGCTGGTGGTGGCGGTACCTGATCTGCACTTCAAACCACC

4.10.1.2. T7 rev. CGGGCTTTGTTAGCAGCCGGATCTCAGTGGTGGTGGTGGTGGTCTCGAGTTATCAGGAGACCGCTAGTTTCAGTTTGTGACCCAGCTTGCTCGGCAGATCGAATAACGCGCAACCGCCACTTCGTGTTGCTCAACGTAGGTCTCTTTATCCGCTTCCTTAATACGCTCCAGACGGTGATCAACATAGTACACACCCGGCATTTTCAGGTTCTTCGCCGGTTTCTTGCTACGATAGGTGGTTTTGAAGTTGCAGATCAGGTGACCGCCACCAACCAGCTTACGCGCATGTCGCTACGGCCCTCCAGGCCACCATCCGCCGGATACAGCATTTCCGTTGTTCCGCTCCCAACCCAGGGTTTCTCTGCATCACCAGGGCCGTTGCTCGGAAAGTTAACACCACGAATCTTCACGTTATAGATCAGGCAGCATCTTGACAGGCTGGTGTCTGGGTGCGGGTCAGAACGCCACCGTCTTCGTAGGTGGTCACACGCTCCAGGTAACCTTCGGGAAGCTCTGTTTAAGAAATCCGGAATGCCCTGGGTGTGGTTGATAAAGGTACGGCTACCGTACATGAAGCTGGTCCGAGAAATATAACGCGAACGGCAGCGGGCCAACCTCAACCACTTTGATACGCATGGTCTGGGTGCCTTCATACGGTTTGCCTTACCCTCGCTGGTGCATTTGAAGTGGTGGTTTACGGTGCCTTCATGTACAGTTTCATGTGCATATCTCCTTAATCAGCTCCTCGCCTTGTCAACCATAC

4.11. Expression and purification of CysPC

BL21-CodonPlus (DE3) RP cells containing the human calpain-1 CysPC gene were grown at 37 °C in kanamycin selective LB media until OD₆₀₀ = 0.6 then induced with 1 mM IPTG. The protein was expressed overnight at 20 °C and cells harvested by centrifugation in a Sorvall RC6 Plus centrifuge (Thermo Fisher Scientific, Inc, MA, USA) using an SLA-3000 rotor at 6080 RCF for 20 min at 4 °C. The cells were re-suspended in 20 mM HEPES, 100 mM NaCl, 0.5 mM TCEP pH 7.6 (buffer A) and lysed by sonication for 5 min (pulsed 5 s on, 10 s off). The lysate was clarified by centrifugation at 4 °C for 40 min at 30,310 RCF in a Sorvall RC6 Plus centrifuge. The supernatant was passed through a 0.2 µm syringe filter and applied to a Ni-NTA column. The bound protein was washed with 15 CV buffer A and eluted with 10 CV buffer A containing 250 mM imidazole, which was further dialyzed in buffer A overnight in a 10 kDa membrane containing 1 mL aliquot of TEV protease. The cleavage product was then passed back through a Ni-NTA column to remove the 6xHis-GB1 solubility tag and TEV protease, with the flow through containing active CysPC as confirmed by SDS-PAGE, mass spectrometry and calpain-1 activity assay.

4.12. Expression and purification of TEV protease

BL21 (DE3) cells containing the TEV gene codon optimised for *E. coli* expression was obtained from Prof. Nigel Richards (Cardiff University).

The cells containing the TEV protease gene were grown at 37 °C in ampicillin selective LB media until OD₆₀₀ = 0.6 then induced with 1 mM IPTG. The protein was expressed overnight at 20 °C and cells harvested by centrifugation in a Sorvall RC6 Plus centrifuge (Thermo Fisher Scientific, Inc, MA, USA) using an SLA-3000 rotor at 6080 RCF for 20 min at 4 °C. The cells were re-suspended in 20 mM HEPES, 100 mM NaCl, 0.5 mM TCEP pH 7.6 (buffer A) and lysed by sonication for 5 min (pulsed 5 s on, 10 s off). The lysate was clarified by centrifugation at 4 °C for 40 min at 30,310 RCF in a Sorvall RC6 Plus centrifuge. The supernatant was passed through a 0.2 µm syringe filter and applied to a Ni-NTA column. The bound protein was washed with 15 CV buffer A and eluted with 10 CV buffer A containing 250 mM imidazole. The eluent was mixed with 20% v/v glycerol (20 mL final volume), and stored at –80 °C in 1 mL aliquots.

Conflicts of interest

The authors declare no competing interests.

Funding sources

LK thanks the IDB Cambridge International Scholarship for support. JCB thanks the EPSRC for funding (doctoral training grants EP/L504749/1 and EP/M50631×/1). This work was financially supported by ERC Starting Grant to AB (No. 336159).

Author contributions

LK and JCB contributed equally to the work. LK wrote this manuscript, developed the original hypothesis for the work, and the computational workflow for the structure-based design of allosteric calpain-1 inhibitors. JCB and CM performed all the experiments to validate the designed ligands. JH provided feedback and helped shape the research. AB, RG, DJM, RKA, conceived the main theme on which the work was performed and ensured that the scientific aspect of the study was rationally valid. All authors read, edited and approved the final manuscript.

Appendix A. Supplementary data

Supplementary data associated with this article can be found in the online version, at <https://doi.org/10.1016/j.ejmech.2018.08.049>. These data include MOL files and InChIKeys of the most important compounds described in this article.

References

- [1] Y. Ono, H. Sorimachi, Calpains - an elaborate proteolytic system, *Biochim. Biophys. Acta Protein Proteonomics* 1824 (2012) 224–236.
- [2] Y. Li, V. Bondada, A. Joshi, J.W. Geddes, Calpain 1 and calpastatin expression is developmentally regulated, *Exp. Neurol.* 220 (2009) 316–319.
- [3] Y. Huang, K.K.W. Wang, The calpain family and human disease, *Trends Mol. Med.* 7 (2001) 355–362.
- [4] Y. Ono, T.C. Saido, H. Sorimachi, Calpain research for drug discovery: challenges and potential, *Nat. Rev. Drug Discov.* 15 (2016) 854–876.
- [5] S.E. Adams, E.J. Robinson, D.J. Miller, P.J. Rizkallah, M.B. Hallett, R.K. Allemann, Conformationally restricted calpain inhibitors, *Chem. Sci.* 6 (2015) 6865–6871.
- [6] Z. Gan-or, G.A. Rouleau, Calpain 1 in neurodegeneration: a therapeutic target? *Lancet Neurol.* 15 (2016) 1118.
- [7] V. Ennes-Vidal, R.F.S. Menna-Barreto, M.H. Branquinho, A.L. Souza Dos Santos, C.M. D'avila-Levy, Why calpain inhibitors are interesting leading compounds to search for new therapeutic options to treat leishmaniasis? *Parasitology* 144 (2017) 117–123.
- [8] K. Kurbatskaya, E.C. Phillips, C.L. Croft, G. Dentoni, M.M. Hughes, M.A. Wade, Al-Sarraj Safa, C. Troakes, M.J.O. Neill, B.G. Perez-Nievas, D.P. Hanger, W. Noble, Upregulation of calpain activity precedes tau phosphorylation and loss of synaptic proteins in Alzheimer's disease brain, *Acta Neuropathol Commun* 4 (2016) 1–15.
- [9] K. Shinohara, M. Tomioka, H. Nakano, S. Toné, H. Ito, S. Kawashima, Apoptosis induction resulting from proteasome inhibition, *Biochem. J.* 317 (1996) 385–388.
- [10] K.K. Wang, R. Nath, A. Posner, K.J. Raser, M. Buroker-Kilgore, I. Hajimohammadreza, A.W. Probert Jr., F.W. Marcoux, Q. Ye, E. Takano, M. Hatanaka, M. Maki, H. Caner, J.L. Collins, A. Fergus, K.S. Lee, E.A. Lunney, S.J. Hays, P. Yuen, An alpha-mercaptoacrylic acid derivative is a selective nonpeptide cell-permeable calpain inhibitor and is neuroprotective, *Proc. Natl. Acad. Sci. U. S. A.* 93 (1996) 6687–6692.
- [11] K.E. Low, S.K. Partha, P.L. Davies, R.L. Campbell, Allosteric inhibitors of calpains: reevaluating inhibition by PD150606 and LSEAL, *Biochim. Biophys. Acta* 1840 (2014) 3367–3373.
- [12] B. Todd, D. Moore, C.C. Deivanayagam, G.D. Lin, D. Chattopadhyay, M. Maki, K.K. Wang, S.V. Narayana, A structural model for the inhibition of calpain by calpastatin: crystal structures of the native domain VI of calpain and its complexes with calpastatin peptide and a small molecule inhibitor, *J. Mol. Biol.* 328 (2003) 131–146.
- [13] S.E. Adams, C. Parr, D.J. Miller, R.K. Allemann, M.B. Hallett, Potent inhibition of Ca²⁺-dependent activation of calpain-1 by novel mercaptoacrylates, *Med Chem Commun* 3 (2012) 566–570.
- [14] S.E. Adams, P.J. Rizkallah, D.J. Miller, E.J. Robinson, M.B. Hallett, R.K. Allemann, The structural basis of differential inhibition of human calpain by indole and phenyl α-mercaptoacrylic acids, *J. Struct. Biol.* 187 (2014) 236–241.
- [15] S. Auvin, B. Pignol, E. Navet, M. Troadec, D. Carre, J. Camara, D. Bigg, P.E. Chabrier, Novel dual inhibitors of calpain and lipid peroxidation with enhanced cellular activity, *Bioorg. Med. Chem. Lett* 16 (2006) 1586–1589.

- [16] P. Kumar, Y.E. Choonara, V. Pillay, In silico affinity profiling of neuroactive polyphenols for post-traumatic calpain inactivation: a molecular docking and atomistic simulation sensitivity analysis, *Molecules* 20 (2015) 135–168.
- [17] L. Lu, M.J. Meehan, S. Gu, Z. Chen, W. Zhang, L. Liu, X. Huang, P.C. Dorrestein, Y. Xu, B.S. Moore, P.Y. Qian, Mechanism of action of thalassospiramides, a new class of calpain inhibitors, *Sci. Rep.* 5 (2015) 1–8.
- [18] M. Siklos, M. BenAissa, G.R.J. Thatcher, Cysteine proteases as therapeutic targets: does selectivity matter? A systematic review of calpain and cathepsin inhibitors, *Acta Pharm. Sin. B* 5 (2015) 506–519.
- [19] T.A. Halgren, R.B. Murphy, R.A. Friesner, H.S. Beard, L.L. Frye, W.T. Pollard, J.L. Banks, Glide: a new approach for rapid, accurate docking and scoring. 2. Enrichment factors in database screening, *J. Med. Chem.* 47 (2004) 1750–1759.
- [20] H.M. Berman, J. Westbrook, Z. Feng, G. Gilliland, T.N. Bhat, H. Weissig, I.N. Shindyalov, P.E. Bourne, The protein data bank, *Nucleic Acids Res.* 28 (2000) 235–242.
- [21] J.B. Baell, G.A. Holloway, New substructure filters for removal of pan assay interference compounds (PAINS) from screening libraries and for their exclusion in bioassays, *J. Med. Chem.* 53 (2010) 2719–2740.
- [22] S.J. Capuzzi, E.N. Muratov, A. Tropsha, Phantom PAINS: problems with the utility of alerts for Pan - assay interference compounds, *J. Chem. Inf. Model.* 57 (2017) 417–427.
- [23] D. Lagorce, O. Sperandio, J.B. Baell, M.A. Miteva, B.O. Villoutreix, FAF-Drugs3: a web server for compound property calculation and chemical library design, *Nucleic Acids Res.* 43 (2015) W200–W207.
- [24] W.W. Busse, S.E. Wenzel, E.O. Meltzer, E.M. Kerwin, M.C. Liu, N. Zhang, Y. Chon, A.L. Budelsky, J. Lin, S.L. Lin, Safety and efficacy of the prostaglandin D2 receptor antagonist AMG 853 in asthmatic patients, *J. Allergy Clin. Immunol.* 131 (2013) 339–345.
- [25] K. Silver, L. Leloup, L.C. Freeman, A. Wells, J.D. Lillich, Non-steroidal anti-inflammatory drugs inhibit calpain activity and membrane localization of calpain 2 protease, *Int. J. Biochem. Cell Biol.* 42 (2010) 2030–2036.
- [26] L. Tong-Jun, Inhibition of Calpain Reduces Allergic Inflammation, 2009, 029751.0 A:1–7.
- [27] P. Jeffrey, S. Summer, Neurobiology of Disease Assessment of the blood – brain barrier in CNS drug discovery, *Neurobiol. Dis.* 37 (2010) 33–37.
- [28] <https://www.aldrichmarketselect.com/> (accessed 2016-10-10).
- [29] G. Madhavi Sastry, M. Adzhigirey, T. Day, R. Annabhimoju, W. Sherman, Protein and ligand preparation: parameters, protocols, and influence on virtual screening enrichments, *J. Comput. Aided Mol. Des.* 27 (2013) 221–234.
- [30] J.C. Shelley, A. Cholleti, L.L. Frye, J.R. Greenwood, M.R. Timlin, M. Uchimaya, Epik: a software program for pKa prediction and protonation state generation for drug-like molecules, *J. Comput. Aided Mol. Des.* 21 (2007) 681–691.
- [31] A. Gaulton, L.J. Bellis, A.P. Bento, J. Chambers, M. Davies, A. Hersey, Y. Light, S. McGlinchey, ChEMBL: a large-scale bioactivity database for drug discovery, *Nucleic Acids Res.* 40 (2011) 1–8.
- [32] Y. Wang, J. Xiao, T.O. Suzek, J. Zhang, J. Wang, Z. Zhou, L. Han, K. Karapetyan, S. Dracheva, B. Shoemaker, E. Bolton, A. Gindulyte, S.H. Bryant, PubChem's BioAssay database, *Nucleic Acids Res.* 40 (2012) D400–D412.
- [33] R Core Team, R: a Language and Environment for Statistical Computing, 2016 version 3.2.4.
- [34] L. Kalash, C. Val, J. Azuaje, M.I. Loza, F. Svensson, A. Zoufir, L. Mervin, G. Ladds, J. Brea, R. Glen, E. Sotelo, A. Bender, Computer-aided design of multi-target ligands at A₁R, A_{2A}R and PDE10A, key proteins in neurodegenerative diseases, *J. Cheminf.* 9 (2017) 1–19.
- [35] ChemAxon Standardizer. <https://www.chemaxon.com/products/standardizer> (accessed 2017-02-27).
- [36] M. Berthold, N. Cebron, F. Dill, KNIME: the Konstanz information miner, *SIGKDD Explor.* 11 (2008) 26–31.
- [37] Wickham Hadley, ggplot2: Elegant Graphics for Data Analysis, 2009.
- [38] SigmaPlot Systat Software, San Jose, CA.
- [39] C. Engler, S. Marillonnet, Combinatorial DNA Assembly Using Golden Gate Cloning, in: K. Polizzi, C. Kontoravdi (Eds.), *Synthetic Biology, Methods in Molecular Biology (Methods and Protocols)*, vol. 1073, Humana Press, Totowa, NJ, 2013.